Letter

Evolution of collectivity and neutron-proton interactions

M. Q. Lin,[1] C. Ma,[1] and Y. M. Zhao[1,2,*]

[1]*Shanghai Key Laboratory of Particle Physics and Cosmology, School of Physics and Astronomy, Shanghai Jiao Tong University, Shanghai 200240, China*

[2]*Collaborative Innovation Center of IFSA (CICIFSA), Shanghai Jiao Tong University, Shanghai 200240, China*

(Received 30 October 2021; accepted 9 February 2022; published 23 February 2022)

In this paper we study the correlation between the evolution of nuclear collective motion and neutron-proton interactions. We construct empirical neutron-proton interactions (denoted by $V_{\rm NP}$) for nuclei in the ($28 < Z < 50$, $50 < N < 82$), ($50 < Z < 82$, $50 < N < 82$), and ($50 < Z < 82$, $82 < N < 126$) major shells. The ratios between $V_{\rm NP}$ and $N_{\rm n}N_{\rm p}$ (the product of valence proton number and valence neutron number) are found to be different for particle-particle, particle-hole, and hole-hole regions of the same major shell, suggesting different average strengths of neutron-proton interactions for these regions. Very interestingly, collective observables of even-even nuclei, e.g., 2^+ and 4^+ state energies, which follow different trajectories in the $N_{\rm n}N_{\rm p}$ scheme for particle-particle, particle-hole, and hole-hole regions, are found to form one *unified and compact* trajectory if those collective observables are plotted in terms of total neutron-proton interactions, $V_{\rm NP}$.

DOI: 10.1103/PhysRevC.105.L021305

The paramount importance of neutron-proton interactions in the evolution of single-particle structure, collectivity, phase shape transitions, and deformation was stressed by de Shalit and Goldhaber [1] and Talmi [2]. In Refs. [3,4], Federman, Pittel, and Campas pointed out that the driving mechanism in the development of nuclear deformation is the proton-neutron interaction between nucleons in spin-orbit partner orbits. If the strength of the proton-neutron interaction is approximately a constant in a considerably large region of one major shell, a very simple quantity, $N_{\rm n}N_{\rm p}$, the product of valence proton number and valence neutron number, could act as a surrogate of the integrated residual neutron-proton interaction of the valence space. Another simple quantity, called the P factor and defined by $P = N_{\rm n}N_{\rm p}/(N_{\rm n} + N_{\rm p})$, could be a reasonable simulation of ratio between the neutron-proton interaction and pairing interaction of the corresponding valence space. In the 1980s Casten and collaborators demonstrated extensively [5–7] that both the $N_{\rm n}N_{\rm p}$ and P-factor schemes provide us with very simple yet very powerful tools to correlate a vast amount of experimental data of the evolution of nuclear collectivity, for instance, the first 2^+ and 4^+ state energies, $E2$ transition rates, and so on, in medium and heavy even-even nuclei. These plots were generalized to odd-even, even-odd, and odd-odd nuclei in Ref. [8].

In the late 1980s, Zhang, Casten, and Brenner extracted the neutron-proton interaction between the last neutron and last proton (denoted by $\delta V_{\rm np}$) based on the experimental atomic masses, as well as the sum of $\delta V_{\rm np}$ over the valence nucleons [9], namely, the total valence neutron-proton interaction (denoted by $V_{\rm NP}$ below). Their results showed the remarkable linearity between $V_{\rm NP}$ and $N_{\rm p}N_{\rm n}$ in the regions of mass number $A \sim 100$ and 130. In Ref. [10] Fu, Jiang, Zhao, and Arima improved the idea of Zhang *et al.* and revisit $V_{\rm NP}$ versus $N_{\rm p}N_{\rm n}$ for three major shells: ($28 < Z < 50$, $50 < N < 82$), ($50 < Z < 82$, $50 < N < 82$), and ($50 < Z < 82$, $82 < N < 126$). By using the AME2003 database [11], Fu *et al.* showed that V_{NP} exhibit excellent linear correlations in terms of $N_{\rm p}N_{\rm n}$ for nuclei with ($28 < Z < 50$, $50 < N < 82$) and ($50 < Z < 82$, $50 < N < 82$). For nuclei with ($50 < Z < 82$, $82 < N < 126$), the linearity remains to be good, in general, except nuclei for $Z = 80$ and 81 which exhibit "slight deviations". Clearly, these evaluations of $V_{\rm NP}$ are limited by the accessibility of experimental atomic-mass data.

For convenience, we repeat here the formula to extract $V_{\rm NP}$ based on atomic masses, presented in Eqs. (4)–(5) of Ref. [10], as follows:

$$V_{\rm NP}(Z,N) = \tfrac{1}{4}\delta_{\rm p}\delta_{\rm n}[S(Z,N) + S(Z_0,N_0) - S(Z_0,N) - S(Z,N_0)], \quad (1)$$

where $\delta_{\rm p}$ ($\delta_{\rm n}$) is $+1$ if the valence protons (neutrons) are particle-like and -1 if the valence protons (neutrons) are hole-like, both Z and N are even numbers, Z_0 (N_0) is the nearest magic number for protons (neutrons), and $S(Z,N)$ is defined by

$$S(Z,N) = B(Z+\delta_{\rm p}, N+\delta_{\rm n}) + B(Z+\delta_{\rm p}, N) + B(Z, N+\delta_{\rm n}) + B(Z,N). \quad (2)$$

Here, B is the nuclear binding energy.

In recent years there have been impressive progresses in predicting atomic masses by extrapolations [12,13], the accuracy of predicted atomic masses is typically 200–400 keV, within three or four steps of extrapolations. As the magnitude of $V_{\rm NP}$ could be 10 or even close to 100 MeV, it is expected to be a good approximation to adopt such predicted atomic

*Corresponding author: ymzhao@sjtu.edu.cn

masses as surrogates of corresponding experimental results in evaluating the results of $V_{\rm NP}$.

Figure 1 plots the values of $V_{\rm NP}$, extracted by using Eqs. (1)–(2), versus $N_{\rm p}N_{\rm n}$, with the AME2020 database [14] as well as extrapolated atomic masses via procedures proposed in Ref. [12], for nuclei in the ($28 < Z < 50$, $50 < N < 82$), ($50 < Z < 82$, $50 < N < 82$), and ($50 < Z < 82$, $82 < N < 126$) major shells, with the constraint that *resultant theoretical uncertainties of $V_{\rm NP}$ are below 1 MeV*. Here, open circles (triangles) correspond to the region in which both valence protons and valence neutrons are particle-like (hole-like), referred to as "particle-particle" ("hole-hole"), open diamonds correspond to the region in which valence neutrons are hole-like while valence protons are particle-like, referred to as "hole-particle", and open squares correspond to the region in which valence neutrons are particle-like while valence protons are hole-like, referred to as "particle-hole". These notations are used throughout this paper. We note that there are many more results of $\delta V_{\rm np}$ (neutron-proton interaction strength $\delta V_{\rm np}$ [9], involving of binding energies for four neighboring even-even nuclei) based on the AME2020 database than those of $V_{\rm NP}$ extracted from nuclear mass database, because, as shown in Eqs. (1)–(2), $V_{\rm NP}$ involves nuclear masses of single-closed nuclei, whose masses are usually not accessible experimentally at present.

In the ($50 < Z < 82$, $50 < N < 82$) major shell, there are rich data for the hole-particle region but few experimental data accessible for other regions of the same major shell. The linear correlation between $V_{\rm NP}$ and $N_{\rm p}N_{\rm n}$ remains to be excellent for $V_{\rm NP}$ values extracted by using theoretically extrapolated atomic masses, as shown in Fig. 1(b). In the ($28 < Z < 50$, $50 < N < 82$) and ($50 < Z < 82$, $82 < N < 126$) major shells, however, one sees different ratios between $V_{\rm NP}$ and $N_{\rm p}N_{\rm n}$ for three different regions of the same major shell, namely, particle-particle, particle-hole, and hole-hole. In Fig. 1(a) one sees sizable differences between the ratio of the particle-particle regions and those of the other two regions of this major shell, hole-hole, and particle-hole; and a very small but systematic difference between the latter two regions is seen, where the ratio of the hole-hole region is very slightly larger. A similar pattern is seen in Fig. 1(c), i.e., the ($50 < Z < 82$, $82 < N < 126$) major shell, in which the differences of the ratios between $V_{\rm NP}$ versus $N_{\rm p}N_{\rm n}$ become much more pronounced, with the ratio of the particle-particle case is the largest, next that of the hole-hole case, and that of the particle-hole is the smallest, among these three regions of the major shell.

The differences of the ratio between $|V_{\rm NP}|$ and $N_{\rm p}N_{\rm n}$ for particle-particle, particle-hole, and hole-hole regions, as exhibited in Fig. 1, suggest that the evolution of collectivity should be different for particle-like and hole-like valence regions of the same major shell. To see whether or not this is indeed the case, in Fig. 2 we plot the first 2^+ energy, denoted by $E_{2_1^+}$ of a few isotones (isotopes) in the ($50 < Z < 82$, $82 < N < 126$) major shell, versus corresponding proton number Z (neutron number N). One sees clearly the asymmetry of $E_{2_1^+}$ values for particle-like and hole-like valence spaces. As the $|V_{\rm NP}|$ values of the particle-particle region are systematically larger than those of the particle-hole region for the same

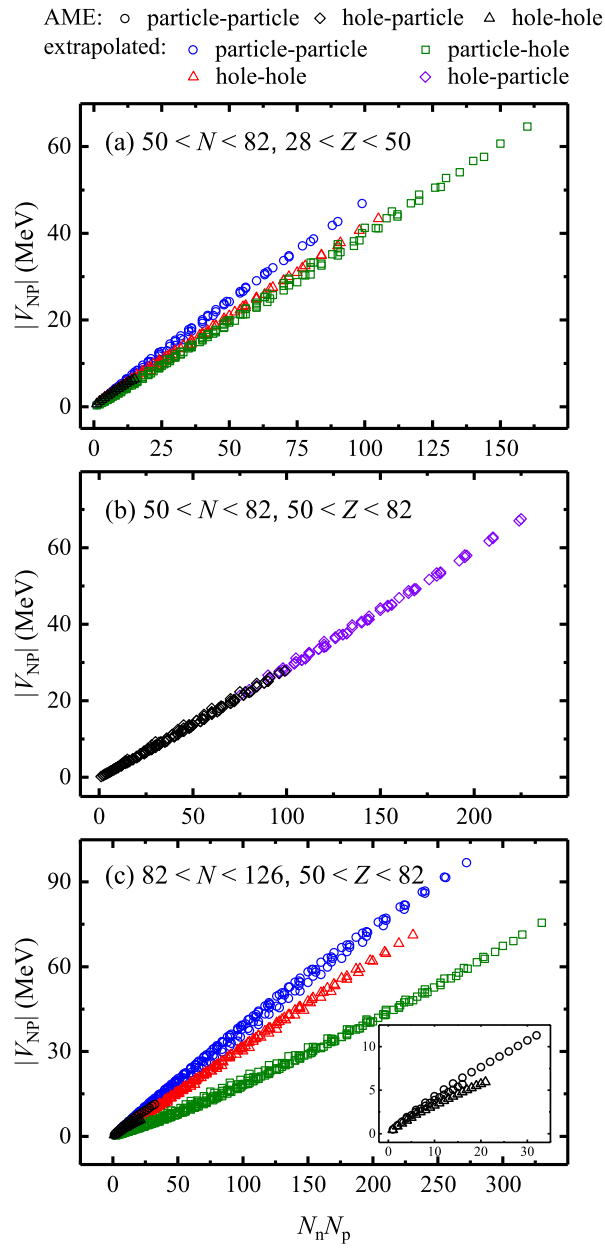

FIG. 1. Integrated neutron-proton interactions $|V_{\rm NP}|$ versus $N_{\rm p}N_{\rm n}$. In panel (a) $28 < Z < 50$ and $50 < N < 82$, in panel (b) $50 < Z < 82$ and $50 < N < 82$, and in panel (c) $50 < Z < 82$ and $82 < N < 126$. Open circles (triangles) correspond to the region in which both valence protons and valence neutrons are particle-like [hole-like], referred to as "particle-particle" ["hole-hole"], open diamonds correspond to the region in which valence neutrons are hole-like while valence protons are particle-like, referred to as "hole-particle", and open squares correspond to the region in which valence neutrons are particle-like while valence protons are hole-like, referred to as "particle-hole". Results extracted from the AME2020 database [14] are in black and those involving predicted atomic masses by extrapolations are in other color – blue, red or green. The sub-panel in (c) is inserted for details of results extracted from experimental atomic masses with small $N_{\rm p}N_{\rm n}$. As *theoretical uncertainties of resultant $|V_{\rm NP}|$ are constrained below 1 MeV*, the error bars of $|V_{\rm NP}|$ are less than the icon size of the results in the figure, and thus are suppressed without any confusion.

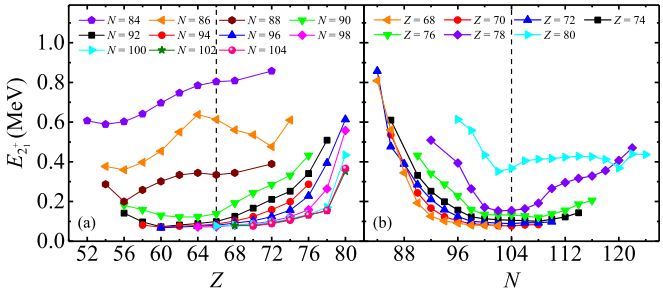

FIG. 2. Values of $E_{2_1^+}$ versus proton number Z and neutron number N, for even-even nuclei in the $(50 < Z < 82,\ 82 < N < 126)$ major shell. (a) $(52 \leqslant Z \leqslant 80,\ 84 \leqslant N \leqslant 104)$, the left hand side of the vertical dotted line corresponds to particle-particle region, and the right hand side corresponds to the particle-hole region. (b) $(68 \leqslant Z \leqslant 80,\ 84 \leqslant N \leqslant 124)$, the left hand side of the vertical dotted line corresponds to the particle-hole region, and the right hand side corresponds to the hole-hole region. Experimental data of $E_{2_1^+}$ are taken from Ref. [15].

values of N_pN_n, one expects that the growth rate of collectivity in the former case is larger, and thus corresponding $E_{2_1^+}$ values are smaller; and this is demonstrated clearly in Fig. 2(a). The same arguments are applicable to results shown in Fig. 2(b), where the $E_{2_1^+}$ values of the hole-hole case are systematically smaller than those of the particle-hole case.

In Ref. [16], Cakirli and collaborators studied the relative values of δV_{np} around the ^{208}Pb nucleus, and in Ref. [17] Cakirli and Casten pointed out, for the first time, the correlation between the differences of the neutron-proton interaction strength and differences in growth rates of collectivity in particle-particle (or hole-hole) and particle-hole regions in the $(50 < Z < 82,\ 82 < N < 126)$ major shell, in terms of $R_{4/2}$ (ratio between $E_{4_1^+}$ and $E_{2_1^+}$) versus N_pN_n. In this paper a consistent pattern of correlation arises. In Figs. 3(a)–3(c), very good correlation between the evolution of $E_{2_1^+}$, $E_{4_1^+}$, or $R_{4/2}$, versus N_pN_n, is seen but *individually for particle-particle, particle-hole, and hole-hole regions*, with a few exceptions to be addressed below (open circles in red, open triangle in blue, and open squares in green). Clearly, the collectivity growth rate of the particle-particle region is the fastest, then that of the hole-hole region, and that of the particle-hole region is the slowest. The pattern of the evolution rates in Figs. 3(a)–3(c) is well consistent with the evolution of V_{NP} versus N_pN_n in Fig. 1(c) as well as the pattern which was first reported in Ref. [17].

Here, it is also worthy to note on "anomalous" results which do not follow a compact correlation in the N_pN_n scheme of Figs. 3(a)–3(c). Those exceptions were also highlighted in Fig. 1 of Ref. [8]. The open circles in red here correspond to nuclei affected by the $Z = 64$ subshell, the effect of which was studied in a number of articles, and here we mention the work by Ogawa and collaborators [18], Casten and collaborators [19], and Scholten [20]. This subshell effect was taken into account by introducing effective valence proton numbers for even-even Ce, Nd, Sm, and Gd isotopes with neutron number N from 84 to 90; and due to the Federman-Pittel mechanism [3,4], the $Z = 64$ subshell effect is negligible for those

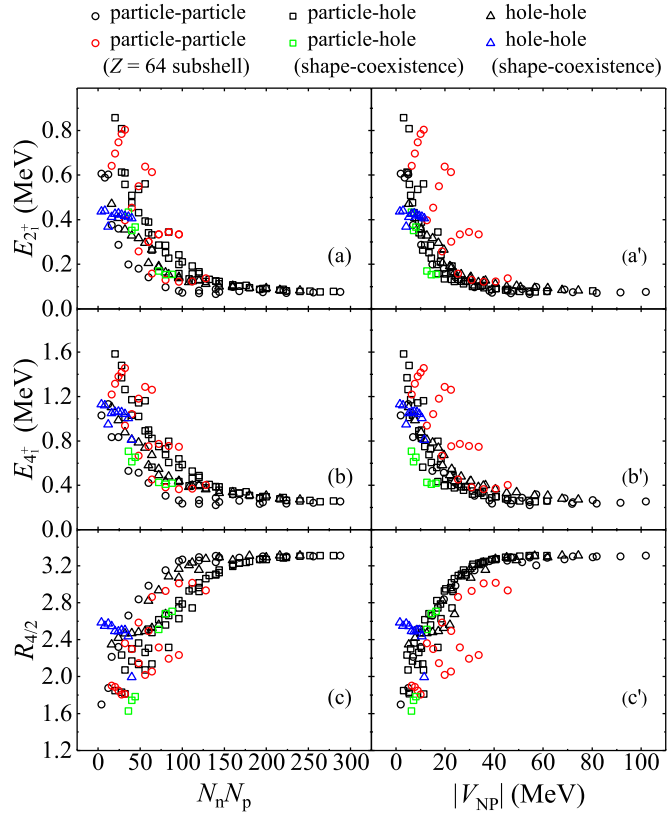

FIG. 3. $E_{2_1^+}$, $E_{4_1^+}$, and $R_{4/2}$ versus N_pN_n and V_{NP} in the $(50 < Z < 82,\ 82 < N < 126)$ major shell. One sees that the different growth rates of given collective observable of even-even nuclei in this major shell for the particle-particle, particle-hole, and hole-hole regions, in the N_pN_n scheme, as plotted in the left hand side panels, are unified to one compact trajectory in the V_{NP} scheme, as plotted in the right hand panels.

isotopes with N larger than 92, as shown by Han and collaborators [21], Zhao and Chen [22], and Fu and collaborators [23]. The open triangles in blue and open squares in green correspond to nuclei with neutron number N close to 104. Such anomalous results were pointed out in Refs. [24–26], and were attributed to coexisting deformed states involving proton excitations across the $Z = 82$ gap when N is close to 104, i.e., the half-filled 82–126 major shell for valence neutrons.

Very interestingly, as shown in Figs. 3(a′)–3(c′), the evolution of $E_{2_1^+}$, $E_{4_1^+}$, or $R_{4/2}$, versus V_{NP} values, follow *one unified and compact* trajectory, for all three regions, particle-particle, particle-hole and hole-hole, throughout the $(50 < Z < 82,\ 82 < N < 126)$ major shell. This is not very surprising, because the strength of the neutron-proton interactions are reasonably taken into account in the integrated V_{NP} values. We note without details that the unification of trajectories, for collective observables such as $E_{2_1^+}$ values of even-even nuclei in this major shell in terms of V_{NP}, for the particle-particle, particle-hole, and hole-hole regions, is found to be robust, if we adopt predicted atomic masses by other theoretical models. This robustness is actually expected, *because the theoretical uncertainties of atomic masses involved here are constrained*

to be below 1 MeV, while the magnitude of $V_{\rm NP}$ can be as large as 100 MeV.

To summarize, in this paper we study the correlation between the evolution of collective motions and integrated neutron-proton interactions. First, we construct total empirical neutron-proton interactions, $V_{\rm NP}$, for nuclei in the $(28 < Z < 50, 50 < N < 82)$, $(50 < Z < 82, 50 < N < 82)$, and $(50 < Z < 82, 82 < N < 126)$ major shells by using atomic mass values. For those with mass data not accessible in the AME2020 database, we make use of the extrapolated mass values with the constraint that resultant theoretical uncertainties of $V_{\rm NP}$ are below 1 MeV.

Second, we report different ratios between $V_{\rm NP}$ and $N_{\rm p}N_{\rm n}$ (the product of valence proton number and valence neutron number), for particle-particle, particle-hole, and hole-hole regions in the $(28 < Z < 50, 50 < N < 82)$ and $(50 < Z < 82, 82 < N < 126)$ major shells. These differences are consistent with asymmetries of $E_{2_1^+}$ results versus proton number or neutron number, for the particle-particle, particle-hole, and hole-hole regions of the $(50 < Z < 82, 82 < N < 126)$ major shell. It is also a reflection of differences of average neutron-proton interaction strength for different regions in one major shell, as discussed in Ref. [16].

Third, we point out the collective observables of even-even nuclei in the $(50 < Z < 82, 82 < N < 126)$ major shell, such as $E_{2_1^+}$, $E_{4_1^+}$, and $R_{4/2}$, which evolve individually in the $N_{\rm p}N_{\rm n}$ scheme for particle-particle, particle-hole, and hole-hole regions in all previous studies, are found to follow *one unified and compact* trajectory, in terms of the values of $V_{\rm NP}$. This new and interesting correlation remains to be robust, if atomic masses predicted by other theoretical models are adopted in evaluating the $V_{\rm NP}$ investigated in this paper.

We thank the National Natural Science Foundation of China (Grants No. 11975151 and No. 11961141003), and MOE Key Lab for Particle Physics, Astrophysics and Cosmology for financial support.

[1] A. De Shalit and M. Goldhaber, Phys. Rev. **92**, 1211 (1953).
[2] I. Talmi, Rev. Mod. Phys. **34**, 704 (1962).
[3] P. Federman and S. Pittel, Phys. Lett. B **69**, 385 (1977); **77**, 29 (1978).
[4] P. Federman, S. Pittel, and R. Campas, Phys. Lett. B **82**, 9 (1979).
[5] R. F. Casten, Phys. Rev. Lett. **54**, 1991 (1985); R. Casten, Nucl. Phys. A **443**, 1 (1985).
[6] R. F. Casten, D. S. Brenner, and P. E. Haustein, Phys. Rev. Lett. **58**, 658 (1987).
[7] R. F. Casten and N. V. Zamfir, J. Phys. G: Nucl. Part. Phys. **22**, 1521 (1996).
[8] Y. M. Zhao, R. F. Casten, and A. Arima, Phys. Rev. Lett. **85**, 720 (2000).
[9] J. Y. Zhang, R. Casten, and D. Brenner, Phys. Lett. B **227**, 1 (1989).
[10] G. J. Fu, H. Jiang, Y. M. Zhao, and A. Arima, Phys. Rev. C **82**, 014307 (2010).
[11] G. Audi, A. H. Wapstra, and C. Thibault, Nucl. Phys. A **729**, 337 (2003); https://www-nds.iaea.org/amdc/ame2003/mass.mas03.
[12] H. Jiang, G. J. Fu, B. Sun, M. Liu, N. Wang, M. Wang, Y. G. Ma, C. J. Lin, Y. M. Zhao, Y. H. Zhang, Z. Ren, and A. Arima, Phys. Rev. C **85**, 054303 (2012).
[13] M. Bao, Z. He, Y. Lu, Y. M. Zhao, and A. Arima, Phys. Rev. C **88**, 064325 (2013); Y. Y. Cheng, Y. M. Zhao, and A. Arima, *ibid.* **90**, 064304 (2014); Z. He, M. Bao, Y. M. Zhao, and A. Arima, *ibid.* **90**, 054320 (2014); M. Bao *et al.*, Sci. China-Phys. Mech. Astron. **60**, 022011 (2017); Y. Y. Cheng *et al.*, J. Phys. G: Nucl. Part. Phys. **44**, 115102 (2017); C. Ma, M. Bao, Z. M. Niu, Y. M. Zhao, and A. Arima, Phys. Rev. C **101**, 045204 (2020).
[14] M. Wang, W. J. Huang, F. G. Kondev *et al.*, Chin. Phys. C **45**, 030003 (2021).
[15] https://www.nndc.bnl.gov/ensdf/.
[16] R. B. Cakirli, D. S. Brenner, R. F. Casten, and E. A. Millman, Phys. Rev. Lett. **94**, 092501 (2005).
[17] R. B. Cakirli and R. F. Casten, Phys. Rev. Lett. **96**, 132501 (2006).
[18] M. Ogawa, R. Broda, K. Zell, P. J. Daly, and P. Kleinheinz, Phys. Rev. Lett. **41**, 289 (1978).
[19] R. F. Casten, D. D. Warner, D. S. Brenner, and R. L. Gill, Phys. Rev. Lett. **47**, 1433 (1981).
[20] O. Scholten, Phys. Lett. B **127**, 144 (1983).
[21] C. S. Han, D. S. Chuu, and S. T. Hsieh, Phys. Rev. C **42**, 280 (1990); D. S. Chuu *et al.*, Nucl. Phys. A **482**, 679 (1988).
[22] Y. M. Zhao and Y. Chen, Phys. Rev. C **52**, 1453 (1995).
[23] G. J. Fu, H. Jiang, Y. M. Zhao, and A. Arima, Phys. Rev. C **84**, 037305 (2011).
[24] Y. M. Zhao, A. Arima, and R. F. Casten, Phys. Rev. C **63**, 067302 (2001).
[25] P. H. Regan, F. R. Xu, P. M. Walker, M. Oi, A. K. Rath, and P. D. Stevenson, Phys. Rev. C **65**, 037302 (2002).
[26] C. E. Vargas, V. Velázquez, and S. Lerma, J. Phys.: Conf. Ser. **578**, 012012 (2015).